Molecular Pharmacology Fast Forward. Published on December 30, 2013 as doi: 10.1124/mol.113.089458
This article has not been copyedited and formatted. The final version may differ from this version.

AMPK Attenuates Adriamycin-Induced Oxidative Podocyte Injury through Thioredoxin-Mediated Suppression of ASK1-P38 Signaling Pathway

Kun Gao, Yuan Chi, Wei Sun, Masayuki Takeda and Jian Yao

Departments of Molecular Signaling (K.G., Y.C., J.Y.), Interdisciplinary Graduate School of Medicine and Engineering, University of Yamanashi, Yamanashi, Japan; Department of Nephrology (K.G., W.S.), Affiliated Hospital of Nanjing University of Chinese Medicine, Nanjing, China; and Department of Urology (M.T.), Interdisciplinary Graduate School of Medicine and Engineering, University of Yamanashi, Yamanashi, Japan

Molecular Pharmacology Fast Forward. Published on December 30, 2013 as DOI: 10.1124/mol.113.089458
This article has not been copyedited and formatted. The final version may differ from this version.

Running title: AMPK attenuates oxidative cell injury

Address correspondence to:

Jian Yao, M.D., Ph.D.,

Department of Molecular Signaling, Interdisciplinary Graduate School of Medicine and Engineering, University of Yamanashi, Chuo, Yamanashi 409-3898, Japan.

Tel/Fax: +81-55-273-8074; E-mail: yao@yamanashi.ac.jp

The numbers:

Text pages, 35

Number of tables, 0

Figures, 7

References, 54

The number of words

Abstract, 246

Introduction, 700

Discussion, 1512

Abbreviation

PX12, 1-methylpropyl 2-imidazolyl disulfide;

AICAR, 5-Aminoimidazole-4-carboxamide ribonucleoside;

AMPK, 5′-adenosine monophosphate-activated protein kinase;

ADR, Adriamycin;

ASK1, Apoptosis signal-regulating kinase 1;

FFA, Flufenamic acid;

GSH, Glutathione;

NAC, N-acetyl-cysteine;

NOX4, NADPH oxidase 4;

ROS, Reactive oxygen species;

$O_2^{\bullet-}$, Superoxide anion;

Trx, Thioredoxin;

TrxR, Thioredoxin Reductase

Molecular Pharmacology Fast Forward. Published on December 30, 2013 as DOI: 10.1124/mol.113.089458
This article has not been copyedited and formatted. The final version may differ from this version.

ABSTRACT

Oxidative stress-induced podocyte injury is one of the major mechanisms underlying the initiation and progression of glomerulosclerosis. AMPK, a serine/threonine kinase that senses intracellular energy status and maintains energy homeostasis, is reported to have anti-oxidative effects. However, little is known about its application and mechanism. In this study, we investigated whether and how AMPK affected oxidative podocyte injury induced by adriamycin (ADR). Exposure of podocytes to ADR resulted in cell injury, which was preceded by increased reactive oxygen species (ROS) generation and P38 activation. Prevention of oxidative stress with the antioxidant N-acetyl-cysteine and glutathione or inhibition of P38 with SB203580 attenuated cell injury. Activation of AMPK with three structurally different AMPK activators also protected podocytes from ADR-elicited cell injury. This effect was associated with strong suppression of oxidative stress-sensitive kinase ASK1 and P38 without obvious influence on ROS level. Further analyses revealed that AMPK promoted thioredoxin (Trx) binding to ASK1. Consistently, AMPK potently suppressed the expression of TXNIP, a negative regulator of Trx, whereas it significantly enhanced the activity of Trx reductases that convert oxidized Trx to reduced form. In further support of a key role of Trx, downregulation or inhibition of Trx exaggerated, whereas downregulation of TXNIP attenuated the cell injury. These results indicate that AMPK prevents oxidative cell injury through Trx-mediated suppression of ASK1-P38 signaling pathway. Our findings thus provide novel mechanistic insights into the antioxidative actions of AMPK. AMPK could be developed as a novel therapeutic target for treatment of oxidative cell injury.

Molecular Pharmacology Fast Forward. Published on December 30, 2013 as DOI: 10.1124/mol.113.089458
This article has not been copyedited and formatted. The final version may differ from this version.

Introduction

Podocytes are highly differentiated glomerular epithelial cells that play an important role in the maintenance of glomerular structure and function. Situated at the special position in glomerulus, podocytes are integrated parts of the glomerular barrier and play a key role in prevention of the leakage of large molecules through size and charge barrier. Podocyte injury leads to proteinuria, which is recognized as an important factor contributing to the initiation and progression of glomerular sclerosis (Kerjaschki, 1994). Podocyte injury has been documented in a variety of renal diseases. Most of them are caused by oxidative stress. Antioxidative therapy has been reported to be effective in attenuation of podocyte injury (Yang et al., 2009). There has been much interest in understanding the molecular mechanisms involved in the regulation of oxidative stresses and developing novel therapeutic approaches against oxidative stress in podocytes.

5′-adenosine monophosphate-activated protein kinase (AMPK) is a serine/threonine protein kinase that acts as an ultra-sensitive sensor monitoring cellular energy status and maintaining cellular energy homeostasis. AMPK is activated under energy stress. Once activated, it turns off ATP consumption and promotes ATP production (Hallows et al., 2010; Mihaylova and Shaw, 2011; Stapleton et al., 1996). Besides its effects on cellular metabolism, AMPK also regulates cellular structure and function. In kidney, AMPK is abundantly expressed and plays an important role in renal pathophysiology. It has been implicated in the control of ion transport, podocyte function, renal hypertrophy, ischemia, inflammation, diabetes and polycystic kidney diseases (Hallows et al., 2010). Several recent studies demonstrated that AMPK protects podocytes from oxidative stress-induced cell injury through suppression of NADPH oxidases (Eid et al., 2010; Piwkowska et al., 2011; Piwkowska et al., 2010; Sharma et al., 2008). However, most of these studies have been done

under the stimulation of high glucose. It is unclear whether AMPK also protects cells from other insult-elicited podocyte injury and whether there are alternative mechanisms implicated in the antioxidative effects of AMPK.

Adriamycin (ADR) is an antitumor agent. It is toxic to many cell types, especially renal cells. This property of ADR has been used for induction of renal cell injury and exploration of molecular mechanisms implicated in proteinuric renal diseases (Okuda et al., 1986). There are growing evidence showing that ADR induces renal injury is through oxidative stress (Morgan et al., 1998; Yang et al., 2009). Using this model, we investigated whether and how AMPK protected podocytes against the toxicity of ADR. Here, we present our results showing that AMPK protect podocytes from oxidative stress-elicited cell injury by potentiation of thioredoxin-mediated suppression of apoptosis signal-regulating kinase 1 (ASK1)-P38 signaling pathway.

Molecular Pharmacology Fast Forward. Published on December 30, 2013 as DOI: 10.1124/mol.113.089458
This article has not been copyedited and formatted. The final version may differ from this version.

Materials and Methods

Materials. PX12 (1-methylpropyl 2-imidazolyl disulfide) was purchased from Santa Cruz Biotechnology (Santa Cruz, CA). Metformin (N, N-Dimethylimidodicarbonimidic diamide) and RPMI 1640 were obtained from Wako Pure Chemical (Osaka, Japan). AICAR (5-Aminoimidazole-4-carboxamide ribonucleoside) was purchased from Cayman Chemical (Ann Arbor, MI). Auranofin [gold (+1) cation; 3,4,5-triacetyloxy-6- (acetyloxymethyl) oxane-2-thiolate; triethylphosphanium] and flufenamic acid (FFA)(2-{[3-(Trifluoromethyl) phenyl] amino} benzoic acid) were purchased from Sigma (Tokyo, Japan). Antibodies against the ASK1 (D11C9), phospho-ASK1 (Thr845), phospho-p38 MAPK (Thr180/Tyr182), phosphor -AMPKα (Thr172), ß-tubulin, caspase-3, thioredoxin 1 (C63C6) and Horseradish peroxidase-conjugated anti-rabbit or mouse IgG were obtained from Cell Signaling Inc (Beverly, MA, USA). Antibody against TXNIP was purchased from MBL International (Woburn, MA). All other chemicals were purchased from Sigma (Tokyo, Japan).

Cells. Murine podocytes were kindly provided by Dr. Karlhans Englich (University of Heidelberg, Heidlberg, German) and cultured as described previously (Saito et al., 2010). For the maintenance and/or propagation, podocytes were cultured with RPMI-1640 medium supplemented with 5% fetal bovine serum (FBS; Sigma Tokyo, Japan) and 1% penicillin-streptomycin in tissue culture flasks in a humidified incubator at 37 °C in an atmosphere of 95% air and 5% carbon dioxide. Assays were performed in the presence of 1% FBS.

Tubular proximal epithelial cell lines, NRK-E52 (from the American Type Culture Collection Collection, Rockville, MD, USA), were maintained in Dulbecco's modified Eagle's medium/F-12 (Gibco-BRL, Gaithersburg, MD, USA) supplemented with 100U/mL penicillin G, 100 mg/mL streptomycin, 0.25 mg/mL amphotericin B and 5% fetal bovine

Molecular Pharmacology Fast Forward. Published on December 30, 2013 as DOI: 10.1124/mol.113.089458
This article has not been copyedited and formatted. The final version may differ from this version.

serum.

Assessment of Cell Viability with WST Reagent. Podocytes were seeded into 96-well cultured plate and allowed to grow for 48 h in RPMI 1640 containing 1% FBS. After that, they were exposed to various stimuli in the presence or absence of the specified inhibitors for indicated time. WST reagent (Dojindo Kumamoto, Japan) was added to each well and incubated for addition 1.5 h before measurement of OD with a spectrometer at the wave of 450 nm. Cell viability was expressed as percentage of control cells.

Detection of $O_2^{\bullet-}$ and ROS Production. The generation of $O_2^{\bullet-}$ and ROS was detected by using a Total ROS/Superoxide Detection Kit from Enzo (Tokyo, Japan) following the manual of the manufacturer (Fang et al., 2011). Briefly, podocytes in 96-well plates were preincubated with $O_2^{\bullet-}$ detection reagent (orange) or oxidative stress detection reagent (green) for 1 h and exposed to various stimulants for an additional 1 h. The immunofluorescent image was visualized and captured using an Olympus IX71 inverted fluorescence microscope (Olympus, Hachioji-shi, Tokyo, Japan) equipped with a standard red and green fluorescence cube. The fluorescence intensity was measured either using NIH ImageJ software (http://rsb.info.nih.gov/ij/) (Murray et al., 2011) or a fluorescence multiwell plate reader (Molecular Devices, Osaka, Japan). According to the manufacture`s product brochure, the kit provides a simple and specific method for detection of comparative levels of total ROS and $O_2^{\bullet-}$ in live cells. Because of the proprietary, the nature of the dyes in the assay kit has not been disclosed.

Assessment of Protein Oxidation. The oxidative modification of proteins was evaluated by OxyBlot™ Protein Oxidation Detection Kit (EMD Millipore) following the manual of the manufacturer. Briefly, the protein lysate was prepared by suspending the prewashed cells in

Molecular Pharmacology Fast Forward. Published on December 30, 2013 as DOI: 10.1124/mol.113.089458
This article has not been copyedited and formatted. The final version may differ from this version.

SDS lysis buffer (62.5mM Tris-HCl, 2%SDS, 10% glycerol) together with freshly added proteinase inhibitor cocktail (Nacalai Tesque, Kyoto, Japan) and 50 mM DTT. 5 μL of protein sample was transferred into eppendorf tubes and was denatured by adding 5 μL of 12% SDS for a final concentration of 6% SDS. The samples were derivatized by adding 10 μL of 1×DNPH solution to each tube. After incubated at room temperature for 15 minutes, 7.5 μL of neutralization solution was added to each tube. Then the samples were subjected to western blotting.

Assessment of Thioredoxin Reductase Activity. The activity of thioredoxin reductase activity was assessed by Cayman's thioredoxin reductase colorimetric assay kit according to the manual of the manufacturer. In brief, cells (1×10^8) were harvested by using a rubber policeman, homogenized by adding 0.75 ml of cold 1×TrxR assay buffer (50 mM potassium phosphate, pH 7.4, containing 1mM EDTA), and centrifuged at 10,000 g for 15 minutes at 4 °C. The supernatants were collected and reacted with NADPH and DTNB. The activities of Trx reductase were calculated by the absorbance at 405 nm.

Transient Transfection of Cells with siRNA. NRK-E52 cells were transiently transfected with siRNA specifically targeting TXNIP and Trx (Rn_Gja1-1 or 5_HP validated siRNA; Qiagen, Japan) or a negative control siRNA (All Stars Negative Control siRNA) at a final concentration of 20 nM using Hyperfect transfection reagent for 48 h. After that, cells were either left untreated or exposed to ADR for the indicated time. Cellular protein was extracted and subjected to Western blot analysis for TXNIP and Trx. Cell viability was evaluated by WST assay.

Propidium Iodide Staining of Cells. NRK-E52 cells were exposed to stimuli for 24h and stained with Propidium diodede (PI) for 5 min according to the protocol provided by the manufacturer (Bio Vision) (Yan et al., 2012). After that, they were subjected to fluorescence

Molecular Pharmacology Fast Forward. Published on December 30, 2013 as DOI: 10.1124/mol.113.089458
This article has not been copyedited and formatted. The final version may differ from this version.

microscopy examination. Cells that are viable are PI positive (red) and indicated necrosis.

Western Blot Analysis. Western blot was performed by the enhanced chemiluminescence system (Yan et al., 2012; Yao et al., 2010). Briefly, extracted cellular proteins were separated by 10% or 12% SDS-polyacrylamide gels and electrotransferred onto polyvinylidine difluoride membranes. After blocking with 3% bovine serum albumin or 5% albumin in PBS, the membranes were incubated with primary antibody (Cell Signaling, Beverly, MA). After washing, the membranes were probed with horseradish peroxidase-conjugated anti-rabbit or anti-mouse IgG (Cell Signaling), and the bands were visualized by the enhanced chemiluminescence system (Amersham Biosciences, Buckinghamshire, UK). The chemiluminescent signal is captured with a Fujifilm luminescent image LAS-1000 analyzer (Fujifilm, Tokyo, Japan) with an exposure time of 3 min and quantified with densitometric software Fujifilm Image Gauge. To confirm equal loading of proteins, the β-tubulin was assayed.

Immunoprecipitation. Podocytes were incubated with 1 mM AICAR or 5 mM metformin for 2 h with or without ADR for an additional of 1.5 h. The cells were lysed in RIPA buffer (50 mM Tris-HCl, 150 mM NaCl, 5 mM EGTA containing 1% Triton, 0.5% deoxycholate, 0.1% SDS). The cellular lysates were homogenated, cleared, and immunoprecipitated using a rabbit polyclonal anti- ASK1 (D11C9) antibody at 4 °C overnight. Immune complexes were precipitated with protein-A／G-sephrose (GE Healthcare, Piscataway, NJ, USA), and washed with RIPA buffer. The resulting pellets were resuspended in 2 × Laemmli buffer, and the proteins were resolved by electrophoresis on a 12% gradient SDS polyacrylamide gel, electrotransferred onto polyvinylidine difluoride membranes, and probed for Trx and ASK1 using the enhanced chemiluminescence system, as described above.

Statistical Analysis. Values are expressed as mean ± S.E. Comparison of two populations

Molecular Pharmacology Fast Forward. Published on December 30, 2013 as DOI: 10.1124/mol.113.089458
This article has not been copyedited and formatted. The final version may differ from this version.

was made by Student t-test. For multiple comparisons, one-way analysis of variance followed by Dunnett's test was employed. Both analyses were done by using the SigmaStat statistical software (Jandel Scientific, San Rafael, CA). $P < 0.05$ was considered to be a statistically significant difference.

Molecular Pharmacology Fast Forward. Published on December 30, 2013 as DOI: 10.1124/mol.113.089458
This article has not been copyedited and formatted. The final version may differ from this version.

Results

Adriamycin Induces Podocyte Injury through Induction of Oxidative stress. Treatment of podocytes with ADR caused an appearance of round-shaped loosely attached cells (Figure 1A). Consistent with the morphological change, ADR caused a concentration-dependent suppression on formazan formation, indicating a loss of cell viability (Figure 1B). Western blot analysis revealed that ADR induced caspase-3 activation, as evidenced by the appearance of a cleaved, low-molecular band of caspase-3 (Figure 1C). These results indicate that ADR induces apoptotic podocyte injury.

To determine the role of oxidative stress in ADR-induced cell injury, we first examined the influence of ADR on reactive oxygen species (ROS) levels. Using fluorescent probers for ROS and superoxide ($O_2^{\bullet -}$), we detected an increased fluorescent intensity in ADR-treated cells, reflecting an elevation in ROS and $O_2^{\bullet -}$ production (Figure 1D, 1E).

Increased ROS level was associated with oxidation of proteins and activation of ROS-sensitive kinases. As shown in Figure 1G, ADR treatment indeed caused a time-dependent increase in protein carbonyl levels, an index of oxidative protein damage, as detected using the DNPH reaction followed by Western blots analysis of the soluble protein fraction. ADR also activated P38 (Figure 1F). Collectively, these results indicate that ADR induces oxidative stress in podocytes.

To assess the role of oxidative stress in ADR-induced cell injury, we evaluated the influence of antioxidant N-acetyl-cysteine (NAC) and glutathione (GSH) on cell viability. As shown in Figure 1H, NAC and GSH potently suppressed the cytotoxic effects of ADR, supporting a mediating role of oxidative stress in the cell injury.

Activation of AMPK Attenuates the Cytotoxic Effects of Adriamycin. AMPK has

Molecular Pharmacology Fast Forward. Published on December 30, 2013 as DOI: 10.1124/mol.113.089458
This article has not been copyedited and formatted. The final version may differ from this version.

recently been reported to have antioxidative effects (Eid et al., 2010; Piwkowska et al., 2011; Piwkowska et al., 2010; Sharma et al., 2008). We therefore tested whether AMPK could attenuate the cytotoxic effects of ADR. For this purpose, we have used three structurally different AMPK activators, which are known to activate AMPK through different signaling mechanisms (Chi et al., 2011; Shaw et al., 2005; Wang et al., 2003). As shown in Figure 2A-2C, AMPK activator 5-Aminoimidazole-4-carboxamide ribonucleoside (AIACR), metformin or flufenamic acid (FFA) all effectively attenuated ADR-induced cell damage, as demonstrated by cell shape change, formazan formation and caspase-3 activation. The effectiveness of these chemicals in induction of AMPK activation was confirmed by the elevated level of AMPK phosphorylation at Thr172 (Fig. 2B, lower panel). In consistence with the protective role of AMPK activators, suppression of AMPK with AMPK inhibitor compound C exaggerated the cytotoxicity of ADR (Fig. 2D). These results thus indicate that AMPK protect podocytes against the cytotoxic effects of ADR.

Given that several recent studies showed that AMPK exerts its anti-oxidative effects through suppression of NADPH oxidase 4 (NOX4) in podocytes (Eid et al., 2010; Piwkowska et al., 2011; Sharma et al., 2008), we examined the influence of AMPK on the generation of superoxide, the major product of NOX4 (Gill and Wilcox, 2006). As shown in Figure 2E, ADR indeed induced $O_2^{\bullet-}$ generation, as revealed by the increased fluorescent intensity in ADR-treated cells. Unexpectedly, in the presence of AMPK activator AICAR or metformin, this effect of ADR was not greatly altered. We also analyzed ROS-induced protein oxidation in the presence or absence of AMPK activators. AMPK also did not affect protein oxidation (Figure 2F). These observations indicate that AMPK does not greatly affect $O_2^{\bullet-}$ level.

Intriguingly, AMPK activators strongly suppressed P38 phosphorylation triggered by ADR

Molecular Pharmacology Fast Forward. Published on December 30, 2013 as DOI: 10.1124/mol.113.089458
This article has not been copyedited and formatted. The final version may differ from this version.

(Figure 3A). As an oxidative stress-sensitive kinase, P38 has been reported to mediate oxidative cell injury both *in vivo* and *in vitro* (Koshikawa et al., 2005; Yan et al., 2012). Here, we also observed that inhibition of P38 with SB203580 significantly attenuated the loss of cell viability induced by ADR (Figure 3B). These observations thus indicate that AMPK might protect podocytes from ADR-induced cell injury through interference of P38 signaling pathway.

AMPK Suppresses Oxidative Stress-Activated ASK1-P38 Pathway. Because P38 is activated by its upstream kinase ASK1 (Hsieh and Papaconstantinou, 2006; Ichijo et al., 1997), we therefore examined the effect of AMPK on ASK1. As shown in Figure 3C, the increased P38 phosphorylation triggered by ADR was preceded by a rapid activation of ASK1. Activation of AMPK with AICAR or metformin suppressed ASK1 in a way similar to P38 (Figure 3D). On the contrary, suppression of AMPK with compound C induced phosphorylation of both ASK1 and P38, and potentiated the activating effect of ADR on these kinases (Figure 3E). These observations thus indicate that AMPK might protect podocyte against the cytotoxity of ADR through suppression of ASK1-P38 signaling pathway.

AMPK Promotes Thioredoxin-ASK1 interaction. Recent studies revealed that ROS-induced activation of ASK1 is negatively regulated by thioredoxin (Trx) through binding to its N-terminal region of ASK1 (Hsieh and Papaconstantinou, 2006; Saitoh et al., 1998). We therefore examined the possible implication of this mechanism. As an initial step toward addressing this speculation, we first established the role of Trx in podocyte injury. As shown in Figure 4A, suppression of Trx with PX12, an irreversible inhibitor of Trx (Kirkpatrick et al., 1998; Wipf et al., 2001), caused a concentration-dependent loss of cell viability, which was also associated with an increased production of ROS (data not shown) and activation of P38 (Figure 4B). Furthermore, PX12 at nontoxic concentration significantly

Molecular Pharmacology Fast Forward. Published on December 30, 2013 as DOI: 10.1124/mol.113.089458
This article has not been copyedited and formatted. The final version may differ from this version.

exaggerated the cytotoxic effect of ADR (Figure 4C). We also looked at the influence of changing redox status of Trx on cell viability. Inhibition of Trx conversion from oxidized form to reduced form through suppression of Trx reductase (TrxR) with auranofin (Cox et al., 2008; Saitoh et al., 1998) also induced a significant loss of cellular viability, as well as an early activation of P38 (Figure 4D, 4E). These observations thus indicate a protective role of Trx in ADR-induced podocyte injury.

We then proceeded to determine whether AMPK activation led to an altered interaction between ASK1 and Trx. For this purpose, we immunoprecipated ASK1 and immunoblotted Trx that bound to ASK1. As shown in Figure 5A, pretreatment of cells with AMPK activator AICAR or metformin markedly enhanced Trx binding to ASK1 under both basal and ADR-stimulated conditions. Interestingly, ADR itself also enhanced Trx binding to ASK1. Western blot analysis of the input used for immunoprecipitation did not detected obvious changes in the levels of ASK1 and Trx (Figure 5B). These results indicate that AMPK promotes Trx binding to ASK1.

Given that there were no obvious changes in Trx levels, we speculated that AMPK might promote the conversion of Trx from inactive oxidized form to active reduced form. To test this speculation, we evaluated the influences of AMPK on the activity of Trx reductase (TrxR) (Saitoh et al., 1998). Figures 5C and 5D show that incubation of podocytes with AMPK activator AICAR or metformin significantly increased the activity of TrxR. We also looked another well-reported regulator of Trx, TXNIP that blocks the reducing activity of Trx and inhibits the interaction between Trx and ASK1 (Li et al., 2009a; Nishiyama et al., 1999; Patwari et al., 2006; Yamawaki et al., 2005). As shown in Figures 5E and 5F, AMPK activator AICAR and metformin potently suppressed TXNIP protein levels. Collectively, these results indicate that AMPK might enhance Trx activities through promotion of TrxR and suppression

Molecular Pharmacology Fast Forward. Published on December 30, 2013 as DOI: 10.1124/mol.113.089458
This article has not been copyedited and formatted. The final version may differ from this version.

of TXNIP.

Implication of Thioredoxin and TXNIP in Adriamycin-Induced Renal Tubular Cell Injury. ADR is also toxic to renal tubular epithelial cells (Lin et al., 2007). We therefore tested whether our findings in podocytes could also be applicable to tubular cells. As shown in Figure 6A-6C, ADR similarly induced cell injury in NRK-E52 cells, a proximal tubular epithelial cell line. Knockdown of Trx with siRNA caused cell damage, as revealed by propidium iodide (PI) staining and formazan formation (Figures 6D-6G), which was also associated with an increased activation of P38 (Figure 6G). Downregulation of Trx also potentiated the cytotoxicity of ADR (Figure 6H). On the contrary, knockdown of TXNIP attenuated the loss of viability and P38 activation induced by ADR (Figures 6I-6K).These data thus reveal an important role of TXNIP/Trx system in oxidative renal cell injury.

Molecular Pharmacology Fast Forward. Published on December 30, 2013 as DOI: 10.1124/mol.113.089458
This article has not been copyedited and formatted. The final version may differ from this version.

Discussion

In this study, we demonstrated that AMPK protected renal cells from ADR-elicited cell injury presumably through Trx-mediated suppression of ASK1-P38 signaling pathway. The molecular mechanisms involved are schematically depicted in Figure 6. Given that oxidative podocyte injury is the major cause for the initiation and progression of proteinuria and glomerular diseases, our finding could have important scientific implications.

ADR is a widely used anticancer drug. However, its clinical use is limited by its toxicity to multiple organs, including heart and kidney (Lin et al., 2007; Okuda et al., 1986). In fact, the toxic mechanism of ADR and its prevention have been the focus of many previous investigations (Granados-Principal et al., 2010; Li et al., 2006; Papeta et al., 2010). Accumulated evidence indicates that ADR induces ROS and causes oxidative cell injury (Morgan et al., 1998; Yang et al., 2009). Consistent with these reports, we confirmed that the toxic effect of ADR on podocytes was closely associated with oxidative stress, as evidenced by the elevated ROS level and protein oxidation. Prevention of oxidative stress with antioxidants or blockade of oxidative stress-sensitive kinase P38 significantly attenuated the cytotoxicity of ADR.

AMPK is reported to have antioxidative actions. Activation of AMPK protects podocytes from high glucose-elicited oxidative injury (Eid et al., 2010; Piwkowska et al., 2011; Piwkowska et al., 2010; Sharma et al., 2008). Here, we demonstrated that three structurally different AMPK activators, AICAR, metformin and FFA, all attenuated podocyte injury. Because these chemicals activate AMPK through different signaling mechanisms (Chi et al., 2011; Shaw et al., 2005; Wang et al., 2003), their effects must be due to activation of AMPK. In further support of this notion, suppression of AMPK with compound C exaggerated ADR-induced activation of ASK1/P38 and loss of cellular viability.

Molecular Pharmacology Fast Forward. Published on December 30, 2013 as DOI: 10.1124/mol.113.089458
This article has not been copyedited and formatted. The final version may differ from this version.

Oxidative stress is defined as an imbalance between prooxidants and antioxidants, resulting in damage to cell by ROS (Jones, 2006). Based on this definition, the classic antioxidative mechanism of AMPK has been focused on re-establishment of the balance through reducing ROS generation and increasing ROS elimination. AMPK inhibits high glucose-induced prooxidant NOX4 expression and $O_2^{\bullet-}$ generation in podocytes (Eid et al., 2010; Piwkowska et al., 2011; Sharma et al., 2008). It also enhances the expression of the antioxidant Trx through promotion of nuclear translocation of Forkhead transcription factor 3 in vascular cells (Hou et al., 2010; Li et al., 2009b). We have examined these parameters in our experimental settings. Our results, however, did not support a causative role of NOX4 in ADR-induced podocyte injury. ADR did not affect NOX4 protein levels (data not shown). The protective effect of AMPK was not associated with a reduced level of $O_2^{\bullet-}$, the major product of NOX4. In addition, AMPK activators also did not affect the protein levels of antioxidant Trx. Thus, AMPK might protect podocytes through mechanisms different from classic scavenging pathways.

ROS causes cell injury through directly oxidizing and damaging DNA, proteins and lipids, as well as by activating several stress-sensitive signaling pathways (Forman et al., 2004; Matsuzawa and Ichijo, 2008). Among many kinases activated by ROS, mitogen-activated protein kinases, P38 and JNK, have been shown to play a key role in oxidative cell injury. Previous studies in podocytes have demonstrated that suppression of P38 attenuates podocyte injury in rat puromycin aminonucleoside nephropathy and mouse ADR nephropathy (Koshikawa et al., 2005; Yan et al., 2012). Consistent with these previous reports, we confirmed the mediating role of P38. Inhibition of P38 with SB203580 significantly attenuated the cytotoxicity of ADR. Interestingly, the protective action of AMPK was also associated with marked suppression of P38 phosphorylation, suggesting that modification of P38 signaling pathway could be involved in the protective effect.

Molecular Pharmacology Fast Forward. Published on December 30, 2013 as DOI: 10.1124/mol.113.089458
This article has not been copyedited and formatted. The final version may differ from this version.

P38 is activated by its upstream kinase ASK1. Similar to P38, ASK1 is also activated by oxidative stress and mediates a wide range of cell responses to oxidative stress (Ichijo et al., 1997; Matsuzawa and Ichijo, 2008). Several studies demonstrated that inhibition of ASK1 abolishes P38 phosphorylation and attenuated oxidative cell injury (Hsieh and Papaconstantinou, 2006; Ichijo et al., 1997). In the current investigation, we observed that P38 activation was preceded by ASK1 activation. Suppression of P38 by AMPK was associated with a reduced level of ASK1 activation. AMPK might protect podocytes from ADR-initiated cell injury through inhibition of ASK1-P38 signaling pathway.

How did AMPK regulate ASK1-P38 signaling pathway? We have focused our attention on Trx, a physiological ASK1 inhibitor that suppresses ASK1 activity and promotes ASK1 degradation through direct binding to the N-terminal region of ASK1 (Hsieh and Papaconstantinou, 2006; Matsuzawa and Ichijo, 2008; Saitoh et al., 1998). It is reported that the increased ROS level activates ASK1 through oxidization and dissociation of Trx from ASK1. Suppression of ASK1 by AMPK could be achieved through promotion and stabilization of the binding. Indeed, activation of AMPK with AICAR and metformin increased the binding. Because this effect of AMPK was not associated with an obvious increase in Trx protein level, maintenance and promotion of Trx in the reduced form could be the mechanism by which AMPK suppressed ASK1 activity. In support of this notion, TrxR, which converts oxidized form of Trx to active reduced form, was significantly enhanced by AMPK. On the contrary, TXNIP, the major negative regulator of Trx that inhibits Trx reducing activities through interaction with redox active domain of Trx, was potently suppressed by AMPK. Furthermore, functional analyses of Trx and TXNIP using specific inhibitor or siRNA confirmed the importance of these molecules in oxidative cell injury. Downregulation or inhibition of Trx sensitized, whereas downregulation of TXNIP blunted cell response to ADR. Of note, the important role of TrxR in prevention of oxidative cell

Molecular Pharmacology Fast Forward. Published on December 30, 2013 as DOI: 10.1124/mol.113.089458
This article has not been copyedited and formatted. The final version may differ from this version.

injury has been previously documented (Andoh et al., 2002; Carvalho et al., 2011; Du et al., 2009; Fang and Holmgren, 2006; Lopert et al., 2012; Lu et al., 2013). Our results thus indicate that increasing Trx reducing activities is the major mechanism behind the antioxidative effect of AMPK.

At present, the mechanisms responsible for the increased activity of TrxR by AMPK are unclear. As for TXNIP, previous studies have demonstrated that AMPK suppresses TXNIP through inhibition of TXNIP transcription and promotion of TXNIP degradation (Wu et al., 2013). The rapidity and potentiality of the suppressive effect of AMPK activators on TXNIP protein levels, as shown in this investigation, suggests that both mechanisms could be involved. It is worth mentioning that TXNIP has also been reported to be able to negatively regulate TrxR activity (Go and Jones, 2010; Lee et al., 2013). Suppression of TXNIP by AMPK might contribute to the increased activities of TrxR.

Of note, previous studies have demonstrated that AMPK reduces high glucose-induced production of ROS in podocytes through suppression of NOX-4 (Eid et al., 2010; Sharma et al., 2008). Here, however, we did not detect a significant change in ROS level. This discrepancy could be due to the different experimental system used for investigation. One recent report described that NOX-2, but NOX-4, is mainly responsible for the increased ROS generation and the toxicity of ADR in cardiac cells (Zhao et al., 2010). Consistently, we observed that the elevated superoxide generation triggered by ADR was not associated with an increased protein level of NOX-4 (data not shown). At present, little information is available regarding AMPK on NOX-2 activities. More detailed studies are needed to clarify the role of AMPK on different isoforms of NADPH oxidases. It is also worth mentioning that the interaction between Trx and ASK1 was, in fact, stimulated by ADR. This phenomenon may be explained by the increased self-defense mechanisms against ROS, including

Molecular Pharmacology Fast Forward. Published on December 30, 2013 as DOI: 10.1124/mol.113.089458
This article has not been copyedited and formatted. The final version may differ from this version.

activation of AMPK (Cardaci et al., 2012; Irrcher et al., 2009; Mungai et al., 2011). Indeed, activation of ASK1 by ADR was transient and was followed by a suppressed ASK1 activities, as compared with control. ROS-induced activation of AMPK, as reported by many investigators (Cardaci et al., 2012; Irrcher et al., 2009; Mungai et al., 2011), should also be able to promote Trx-ASK1 interaction. We have also tried to confirm the role of AMPK by using genetic approaches. Unfortunately, podocytes we used were difficult to be transfected, which we have described in our previous report (Yan et al., 2012).

Our finding could have significant implications. First, both Trx and ASK1 have been reported to be critically involved in the pathological situations, like inflammation, tumor, neurodegeneration, aging, and cell injury (Al-Gayyar et al., 2011; Matsuzawa and Ichijo, 2008). The importance of AMPK in these pathological situations has also been well documented (Cardaci et al., 2012; Hallows et al., 2010). It is possible that the action of AMPK might be through modification of ASK1-Trx interaction. Second, our results indicate that AMPK might be targeted to enhance or attenuate the toxicity of ADR. Depending on the context, it might be used to potentiate the tumor-killing efficacy of ADR or to protect the cells from the toxicity of ADR.

Collectively, our study demonstrated a protective effect of AMPK on ADR-induced renal cell injury through Trx-mediated suppression of ASK1-P38 signaling pathway. Our findings thus provide novel mechanistic insights into the actions of AMPK. AMPK might be a promising therapeutic target for prevention of oxidative podocyte injury.

Molecular Pharmacology Fast Forward. Published on December 30, 2013 as DOI: 10.1124/mol.113.089458
This article has not been copyedited and formatted. The final version may differ from this version.

Acknowledgments

We thank Dr. Masanori Kitamura (University of Yamanashi, Japan) for his helpful contributions and discussions.

Authorship Contributions

Participated in research design: Yao, Gao, and Takeda

Conducted experiments: Gao, Chi, and Sun.

Performed data analysis: Gao, Chi, Sun, Takeda, and Yao

Wrote or contributed to the writing of the manuscript: Gao, Yao

References

Al-Gayyar MM, Abdelsaid MA, Matragoon S, Pillai BA and El-Remessy AB (2011) Thioredoxin interacting protein is a novel mediator of retinal inflammation and neurotoxicity. *Br J Pharmacol* **164**(1): 170-180.

Andoh T, Chock PB and Chiueh CC (2002) The roles of thioredoxin in protection against oxidative stress-induced apoptosis in SH-SY5Y cells. *J Biol Chem* **277**(12): 9655-9660.

Cardaci S, Filomeni G and Ciriolo MR (2012) Redox implications of AMPK-mediated signal transduction beyond energetic clues. *J Cell Sci* **125**(Pt 9): 2115-2125.

Carvalho CML, Lu J, Zhang X, Arner ESJ and Holmgren A (2011) Effects of selenite and chelating agents on mammalian thioredoxin reductase inhibited by mercury: implications for treatment of mercury poisoning. *FASEB J* **25**(1): 370-381.

Chi Y, Li K, Yan QJ, Koizumi S, Shi LY, Takahashi S, Zhu Y, Matsue H, Takeda M, Kitamura M and Yao J (2011) Nonsteroidal anti-inflammatory drug flufenamic acid is a potent activator of AMP-activated protein kinase. *J Pharmacol Exp Ther* **339**(1): 257-266.

Cox AG, Brown KK, Arner ESJ and Hampton MB (2008) The thioredoxin reductase inhibitor auranofin triggers apoptosis through a Bax/Bak-dependent process that involves peroxiredoxin 3 oxidation. *Biochem Pharmacol* **76**(9): 1097-1109.

Du YT, Wu YF, Cao XL, Cui W, Zhang HH, Tian WX, Ji MJ, Holmgren A and Zhong LW (2009) Inhibition of mammalian thioredoxin reductase by black tea and its constituents: Implications for anticancer actions. *Biochimie* **91**(3): 434-444.

Eid AA, Ford BM, Block K, Kasinath BS, Gorin Y, Ghosh-Choudhury G, Barnes JL and Abboud HE (2010) AMP-activated protein kinase (AMPK) negatively regulates Nox4-dependent activation of p53 and epithelial cell apoptosis in diabetes. *J Biol Chem* **285**(48): 37503-37512.

Fang JG and Holmgren A (2006) Inhibition of thioredoxin and thioredoxin reductase by

4-hydroxy-2-nonenal in vitro and in vivo. *J Am Chem Soc* **128**(6): 1879-1885.

Fang X, Huang T, Zhu Y, Yan QJ, Chi Y, Jiang JX, Wang PY, Matsue H, Kitamura M and Yao J (2011) Connexin43 hemichannels contribute to cadmium-induced oxidative stress and cell injury. *Antioxid Redox Signal* **14**(12): 2427-2439.

Forman HJ, Fukuto JM and Torres M (2004) Redox signaling: thiol chemistry defines which reactive oxygen and nitrogen species can act as second messengers. *Am J Physiol Cell Physiol* **287**(2): C246-C256.

Gill PS and Wilcox CS (2006) NADPH oxidases in the kidney. *Antioxid Redox Signal* **8**(9-10): 1597-1607.

Go YM and Jones DP (2010) Redox Control Systems in the nucleus: mechanisms and functions. *Antioxid Redox Signal* **13**(4): 489-509.

Granados-Principal S, Quiles JL, Ramirez-Tortosa CL, Sanchez-Rovira P and Ramirez-Tortosa M (2010) New advances in molecular mechanisms and the prevention of adriamycin toxicity by antioxidant nutrients. *Food Chem Toxicol* **48**(6): 1425-1438.

Hallows KR, Mount PF, Pastor-Soler NM and Power DA (2010) Role of the energy sensor AMP-activated protein kinase in renal physiology and disease. *Am J Physiol Renal Physiol* **298**(5): F1067-F1077.

Hou X, Song J, Li XN, Zhang L, Wang X, Chen L and Shen YH (2010) Metformin reduces intracellular reactive oxygen species levels by upregulating expression of the antioxidant thioredoxin via the AMPK-FOXO3 pathway. *Biochem Biophys Res Commun* **396**(2): 199-205.

Hsieh CC and Papaconstantinou J (2006) Thioredoxin-ASK1 complex levels regulate ROS-mediated p38 MAPK pathway activity in livers of aged and long-lived Snell dwarf mice. *FASEB J* **20**(2): 259-268.

Ichijo H, Nishida E, Irie K, ten Dijke P, Saitoh M, Moriguchi T, Takagi M, Matsumoto K,

Miyazono K and Gotoh Y (1997) Induction of apoptosis by ASK1, a mammalian MAPKKK that activates SAPK/JNK and p38 signaling pathways. *Science* **275**(5296): 90-94.

Irrcher I, Ljubicic V and Hood DA (2009) Interactions between ROS and AMP kinase activity in the regulation of PGC-1alpha transcription in skeletal muscle cells. *Am J Physiol Cell Physiol* **296**(1): C116-123.

Jones DP (2006) Redefining oxidative stress. *Antioxid Redox Signal* **8**(9-10): 1865-1879.

Kerjaschki D (1994) Dysfunctions of cell biological mechanisms of visceral epithelial cell (podocytes) in glomerular diseases. *Kidney Int* **45**(2): 300-313.

Kirkpatrick DL, Kuperus M, Dowdeswell M, Potier N, Donald LJ, Kunkel M, Berggren M, Angulo M and Powis G (1998) Mechanisms of inhibition of the thioredoxin growth factor system by antitumor 2-imidazolyl disulfides. *Biochem Pharmacol* **55**(7): 987-994.

Koshikawa M, Mukoyama M, Mori K, Suganami T, Sawai K, Yoshioka T, Nagae T, Yokoi H, Kawachi H, Shimizu F, Sugawara A and Nakao K (2005) Role of p38 mitogen-activated protein kinase activation in podocyte injury and proteinuria in experimental nephrotic syndrome. *J Am Soc Nephrol* **16**(9): 2690-2701.

Lee S, Kim SM and Lee RT (2013) Thioredoxin and thioredoxin target proteins: from molecular mechanisms to functional significance. *Antioxid Redox Signal* **18**(10): 1165-1207.

Li JH, Deane JA, Campanale NV, Bertram JF and Ricardo SD (2006) Blockade of p38 mitogen-activated protein kinase and TGF-beta 1/Smad signaling pathways rescues bone marrow-derived peritubular capillary endothelial cells in adriamycin-induced nephrosis. *J Am Soc Nephrol* **17**(10): 2799-2811.

Li X, Rong Y, Zhang M, Wang XL, LeMaire SA, Coselli JS, Zhang Y and Shen YH (2009a) Up-regulation of thioredoxin interacting protein (Txnip) by p38 MAPK and FOXO1

contributes to the impaired thioredoxin activity and increased ROS in glucose-treated endothelial cells. *Biochem Biophys Res Commun* **381**(4): 660-665.

Li XN, Song J, Zhang L, LeMaire SA, Hou X, Zhang C, Coselli JS, Chen L, Wang XL, Zhang Y and Shen YH (2009b) Activation of the AMPK-FOXO3 pathway reduces fatty acid-induced increase in intracellular reactive oxygen species by upregulating thioredoxin. *Diabetes* **58**(10): 2246-2257.

Lin H, Hou CC, Cheng CF, Chiu TH, Hsu YH, Sue YM, Chen TH, Hou HH, Chao YC, Cheng TH and Chen CH (2007) Peroxisomal proliferator-activated receptor-alpha protects renal tubular cells from doxorubicin-induced apoptosis. *Mol Pharmacol* **72**(5): 1238-1245.

Lopert P, Day BJ and Patel M (2012) Thioredoxin reductase deficiency potentiates oxidative stress, mitochondrial dysfunction and cell death in dopaminergic cells. *PloS One* **7**(11).

Lu J, Vlamis-Gardikas A, Kandasamy K, Zhao R, Gustafsson TN, Engstrand L, Hoffner S, Engman L and Holmgren A (2013) Inhibition of bacterial thioredoxin reductase: an antibiotic mechanism targeting bacteria lacking glutathione. *FASEB J* **27**(4): 1394-1403.

Matsuzawa A and Ichijo H (2008) Redox control of cell fate by MAP kinase: physiological roles of ASK1-MAP kinase pathway in stress signaling. *Biochim Biophys Acta* **1780**(11): 1325-1336.

Mihaylova MM and Shaw RJ (2011) The AMPK signalling pathway coordinates cell growth, autophagy and metabolism. *Nat Cell Biol* **13**(9): 1016-1023.

Morgan WA, Kaler B and Bach PH (1998) The role of reactive oxygen species in adriamycin and menadione-induced glomerular toxicity. *Toxicol Lett* **94**(3): 209-215.

Mungai PT, Waypa GB, Jairaman A, Prakriya M, Dokic D, Ball MK and Schumacker PT (2011) Hypoxia triggers AMPK activation through reactive oxygen species-mediated activation of calcium release-activated calcium channels. *Mol Cell Biol* **31**(17): 3531-3545.

Murray JW, Thosani AJ, Wang PJ and Wolkoff AW (2011) Heterogeneous accumulation of fluorescent bile acids in primary rat hepatocytes does not correlate with their homogenous expression of ntcp. *Am J Physiol Gastrointest Liver Physiol* **301**(1): G60-G68.

Nishiyama A, Matsui M, Iwata S, Hirota K, Masutani H, Nakamura H, Takagi Y, Sono H, Gon Y and Yodoi J (1999) Identification of thioredoxin-binding protein-2/vitamin D(3) up-regulated protein 1 as a negative regulator of thioredoxin function and expression. *J Biol Chem* **274**(31): 21645-21650.

Okuda S, Oh Y, Tsuruda H, Onoyama K, Fujimi S and Fujishima M (1986) Adriamycin-induced nephropathy as a model of chronic progressive glomerular disease. *Kidney Int* **29**(2): 502-510.

Papeta N, Zheng Z, Schon EA, Brosel S, Altintas MM, Nasr SH, Reiser J, D'Agati VD and Gharavi AG (2010) Prkdc participates in mitochondrial genome maintenance and prevents adriamycin-induced nephropathy in mice. *J Clin Invest* **120**(11): 4055-4064.

Patwari P, Higgins LJ, Chutkow WA, Yoshioka J and Lee RT (2006) The interaction of thioredoxin with Txnip. Evidence for formation of a mixed disulfide by disulfide exchange. *J Biol Chem* **281**(31): 21884-21891.

Piwkowska A, Rogacka D, Jankowski M and Angielski S (2011) Extracellular ATP through P2 receptors activates AMP-activated protein kinase and suppresses superoxide generation in cultured mouse podocytes. *Exp Cell Res* **317**(13): 1904-1913.

Piwkowska A, Rogacka D, Jankowski M, Dominiczak MH, Stepinski JK and Angielski S (2010) Metformin induces suppression of NAD(P)H oxidase activity in podocytes. *Biochem Biophys Res Commun* **393**(2): 268-273.

Saito Y, Okamura M, Nakajima S, Hayakawa K, Huang T, Yao J and Kitamura M (2010) Suppression of nephrin expression by TNF-alpha via interfering with the cAMP-retinoic acid receptor pathway. *Am J Physiol Renal Physiol* **298**(6): F1436-F1444.

Saitoh M, Nishitoh H, Fujii M, Takeda K, Tobiume K, Sawada Y, Kawabata M, Miyazono K and Ichijo H (1998) Mammalian thioredoxin is a direct inhibitor of apoptosis signal-regulating kinase (ASK) 1. *EMBO J* **17**(9): 2596-2606.

Sharma K, Ramachandrarao S, Qiu G, Usui HK, Zhu Y, Dunn SR, Ouedraogo R, Hough K, McCue P, Chan L, Falkner B and Goldstein BJ (2008) Adiponectin regulates albuminuria and podocyte function in mice. *J Clin Invest* **118**(5): 1645-1656.

Shaw RJ, Lamia KA, Vasquez D, Koo SH, Bardeesy N, Depinho RA, Montminy M and Cantley LC (2005) The kinase LKB1 mediates glucose homeostasis in liver and therapeutic effects of metformin. *Science* **310**(5754): 1642-1646.

Stapleton D, Mitchelhill KI, Gao G, Widmer J, Michell BJ, Teh T, House CM, Fernandez CS, Cox T, Witters LA and Kemp BE (1996) Mammalian AMP-activated protein kinase subfamily. *J Biol Chem* **271**(2): 611-614.

Wang W, Yang X, Lopez de Silanes I, Carling D and Gorospe M (2003) Increased AMP:ATP ratio and AMP-activated protein kinase activity during cellular senescence linked to reduced HuR function. *J Biol Chem* **278**(29): 27016-27023.

Wipf P, Hopkins TD, Jung JK, Rodriguez S, Birmingham A, Southwick EC, Lazo JS and Powis G (2001) New inhibitors of the thioredoxin-thioredoxin reductase system based on a naphthoquinone spiroketal natural product lead. *Bioorg Med Chem Lett* **11**(19): 2637-2641.

Wu N, Zheng B, Shaywitz A, Dagon Y, Tower C, Bellinger G, Shen CH, Wen J, Asara J, McGraw TE, Kahn BB and Cantley LC (2013) AMPK-dependent degradation of TXNIP upon energy stress leads to enhanced glucose uptake via GLUT1. *Mol Cell* **49**(6): 1167-1175.

Yamawaki H, Pan S, Lee RT and Berk BC (2005) Fluid shear stress inhibits vascular inflammation by decreasing thioredoxin-interacting protein in endothelial cells. *J Clin*

Invest **115**(3): 733-738.

Yan Q, Gao K, Chi Y, Li K, Zhu Y, Wan Y, Sun W, Matsue H, Kitamura M and Yao J (2012) NADPH oxidase-mediated upregulation of connexin43 contributes to podocyte injury. *Free Radic Biol Med* **53**(6): 1286-1297.

Yang L, Zheng SR and Epstein PN (2009) Metallothionein over-expression in podocytes reduces adriamycin nephrotoxicity. *Free Radic Res* **43**(2): 174-182.

Yao J, Huang T, Fang X, Chi Y, Zhu Y, Wan YG, Matsue H and Kitamura M (2010) Disruption of gap junctions attenuates aminoglycoside-elicited renal tubular cell injury. *Br J Pharmacol* **160**(8): 2055-2068.

Zhao Y, McLaughlin D, Robinson E, Harvey AP, Hookham MB, Shah AM, McDermott BJ and Grieve DJ (2010) Nox2 NADPH oxidase promotes pathologic cardiac remodeling associated with Doxorubicin chemotherapy. *Cancer Res* **70**(22): 9287-9297.

Molecular Pharmacology Fast Forward. Published on December 30, 2013 as DOI: 10.1124/mol.113.089458
This article has not been copyedited and formatted. The final version may differ from this version.

Footnote

This work was supported by Grants-in-Aid for Scientific Research from the Ministry of Education, Culture, Sports, Science and Technology, Japan [17659255 and 20590953].

Molecular Pharmacology Fast Forward. Published on December 30, 2013 as DOI: 10.1124/mol.113.089458
This article has not been copyedited and formatted. The final version may differ from this version.

Legends

Figure 1. Adriamycin induces podocyte injury through induction of oxidative stress. (A) Induction of cell shape change by ADR. Podocytes were exposed to the indicated concentrations of ADR for 24 h. Cell morphology was photographed using phase-contrast microscopy (Magnification, ×100). (B) Effect of ADR on cell viability. Podocytes in 96-well plates were exposed to the indicated concentrations of ADR for 24 h. The cell viability was evaluated by WST assay. Data are expressed as percentage of living cells against the untreated control (mean ± SE, n = 4). *P < 0.05, #P < 0.01 *versus* zero point. (C) Activation of caspase-3 by ADR. Podocytes were exposed to the indicated concentration of ADR for 12 h and subjected to Western blot analysis of caspase-3. The top band represents procaspase-3 (Mr 35,000) and the bottom band indicates its cleaved, mature form (Mr 17,000). (D, E) Effects of ADR on $O_2^{\bullet -}$ and ROS production. Podocytes were loaded with $O_2^{\bullet -}$ and ROS detection reagent for 1 h and stimulated with 1 μg/ml ADR for the indicated time intervals (D) or the indicated concentrations of ADR for 4.5 h (E). After that, they were subjected to fluorescent microscopy (Magnification, ×400). Quantitative measurements of the fluorescence intensities were done using ImageJ 1.46 software. Densitometric analyses of ROS or superoxide are shown at the bottom of the figure. The data were expressed as percentage relative to untreated control (mean ± SE, n = 3; * P < 0.05 *versus* control). (F) Induction of P38 phosphorylation by ADR. Podocytes were incubated with various concentrations of ADR for 12 h. Cellular lysates were subjected to Western blot analysis for phosphorylated P38. (G) Induction of oxidative modification of proteins by ADR. Podocytes were exposed to 1μg/ml ADR for the indicated time intervals and then subjected to OxyBlot™ Protein Oxidation Detection Kit and immunodetection of carbonyl groups. (H) Effect of antioxidants on cell viability. Podocytes were exposed to the indicated concentrations of ADR for 24 h in the presence or absence of antioxidants (10 mM GSH and

Molecular Pharmacology Fast Forward. Published on December 30, 2013 as DOI: 10.1124/mol.113.089458
This article has not been copyedited and formatted. The final version may differ from this version.

5 mM NAC). The cell viability was evaluated by WST assay. Data are expressed as percentage of living cells against the untreated control (mean ± SE, n = 4; # $P < 0.01$ *versus* ADR alone).

Figure 2. Activation of AMPK attenuates the cytotoxic effects of Adriamycin. (A) Effects of AMPK activators on cell morphology. Podocytes were exposed to 1 μg/ml ADR with or without AMPK activators (1 mM AICAR, 5 mM Metformin or 50 μM FFA) for 24 h. Cell morphology was photographed using phase-contrast microscopy (Magnification, ×100). (B) Effect of AMPK activators on cell viability and AMPK activation. Podocytes were exposed to the indicated concentrations of ADR for 24 h in the presence or absence of AMPK activators (1 mM AICAR, 5 mM Metformin or 50 μM FFA). The cell viability was evaluated by WST assay (upper panel). Data are expressed as percentage of living cells against the untreated control (mean ± SE, n = 4; * $P < 0.05$ *versus* ADR alone). Podocytes were incubated with the aforementioned AMPK activators for 1 h and cellular lysates were subjected to Western blot analysis of phosphorylated AMPK and β-tubulin (lower panel). (C) Effects of AMPK activators on caspase-3 activation. Podocytes were exposed to 1 μg/ml ADR for 12 h with or without AMPK activator (1 mM AICAR and 5 mM metformin) and subjected to Western blot analysis of caspase-3. The top band represents procaspase-3 (Mr 35,000) and the bottom band indicates its cleaved, mature form (Mr 17,000). (D) Effect of AMPK inhibitor on cell viability. Podocytes were exposed to the indicated concentrations of ADR in the presence or absence of AMPK inhibitor compound C (30 μM) for 24 h. The cell viability was evaluated by WST assay. Data are expressed as percentage of living cells against the untreated control (mean ± SE, n = 4; # $P < 0.01$ versus ADR alone). (E) Effect of AMPK activators on $O_2^{\bullet -}$ and ROS production induced by ADR. Podocytes were loaded with $O_2^{\bullet -}$ and ROS detection reagent in the presence or absence of AMPK activators (1 mM AICAR and 5 mM metformin) for 1 h and exposed to 1μg/ml ADR for an additional 4 h. After that, they were subjected to fluorescent microscopy (Magnification, ×400). Densitometric analyses of $O_2^{\bullet -}$ production was shown at the bottom. Quantitative measurements of the fluorescence intensities were done using Image J software. Data are expressed as relative intensity against zero point control (mean ± SE, n = 3; * $P < 0.05$ *versus* respective control). (F) Effects of AMPK activators on oxidative modification of proteins stimulated by ADR. Podocytes were incubated with or without AMPK activators (1 mM AICAR and 5 mM Metformin) for 2 h and exposed to 1 μg/ml ADR for another 3 h and

Molecular Pharmacology Fast Forward. Published on December 30, 2013 as DOI: 10.1124/mol.113.089458
This article has not been copyedited and formatted. The final version may differ from this version.

then subjected to OxyBlot™ Protein Oxidation Detection Kit and immunodetection of carbonyl groups. Arrows denote ADR-treated cells.

Figure 3. AMPK suppresses oxidative stress-elicited activation of ASK1-p38 pathway. (A) Effects of AMPK activators on activation of P38 by ADR. Podocytes were incubated with 1 mM AICAR or 5 mM metformin for 1 h before exposing to various concentrations of ADR for an additional of 12 h. Cellular lysates were subjected to Western blot analysis for phosphorylated P38. Results are representatives of at least 3 separate experiments. Densitometric analyses of phosphorylated P38 at 1 μg/ml ADR are shown at the bottom. Data are expressed as percentage of the untreated control (mean ± SE, n = 3; # $P<0.05$ compared with the untreated control; * $P < 0.05$). (B) Effect of P38 inhibitor on cell viability. Podocytes were exposed to the indicated concentrations of ADR for 24 h in the presence or absence of 10 μM SB203580. The cell viability was evaluated by WST assay. Data are expressed as percentage of living cells against the untreated control (mean ± SE, n = 4; *$P < 0.05$ *versus* ADR alone). (C) Induction of ASK1 and P38 phosphorylation by ADR. Podocytes were incubated with 1 μg/ml ADR for indicated time intervals. Cellular lysates were subjected to Western blot analysis for phosphorylated ASK1 and P38. Results are representatives of at least 3 separate experiments. Densitometric analyse of phosphorylated ASK1 is shown at the bottom. Data are expressed as percentage of control (mean ± SE, n = 3; * $P < 0.05$ compared with control). (D) Suppression of ADR-induced ASK1 activation by AMPK activators. Podocytes were incubated with 1 mM AICAR and 5 mM metformin for 1 h and exposed to 1 μg/ml ADR for another 45 min. Cellular lysates were subjected to Western blot analysis for phosphorylated ASK1. Results are representatives of at least 3 separate experiments. Densitometric analyse of phosphorylated ASK1 is shown at the bottom. Data are expressed as percentage of ADR-free control (mean ± SE, n = 3; # $P < 0.05$ compared with the untreated control; * $P < 0.05$). (E) Induction of ASK1 and P38 activation by AMPK inhibitor compound

Molecular Pharmacology Fast Forward. Published on December 30, 2013 as DOI: 10.1124/mol.113.089458
This article has not been copyedited and formatted. The final version may differ from this version.

C. Podocytes were incubated with 30 μM compound C for 1 h and exposed to 1 μg/ml ADR for 45 min (upper panel, ASK1) or 6 h (lower panel, P38), respectively. Cellular lysates were subjected to Western blot analysis for phosphorylated ASK1 and P38.

Figure 4. Regulation of cell viability and P38 activation by thioredoxin. (A) Effect of PX12 on cell viability. Podocytes were exposed to various concentrations of PX12 for 24 h. The cell viability was evaluated by WST assay. Data are expressed as percentage of living cells against the untreated control (mean ± SE, n = 4; *P < 0.05 *versus* zero point). (B) Induction of P38 activation by PX12. Podocytes were incubated with various concentrations of Px12 for 3 h. Cellular lysates were subjected to Western blot analysis for phosphorylated P38. (C) Exaggeration of ADR-triggered loss of cell viability by PX12. Podocytes in 96-well plates were exposed to various concentrations of ADR with or without 10 μM PX12 for 24 h. The cell viability was evaluated by WST assay. Data are expressed as percentage of living cells against the untreated control (mean ± SE, n = 4; # P < 0.01 *versus* respective control). (D) Effect of auranofin on cell viability. Podocytes were exposed to various concentrations of auranofin for 6 h. The cell viability was evaluated by WST assay. Data are expressed as percentage of living cells against the untreated control (mean ± SE, n = 4; # < 0.01 *versus* zero point). (E) Induction of P38 phosphorylation by auranofin. Podocytes were incubated with 0.2 μm auranofin for the indicated time intervals. Cellular lysates were subjected to Western blot analysis for phosphorylated level of P38.

Figure 5. AMPK promotes thioredoxin-ASK1 interaction. (A) Effects of AMPK activators on binding of Trx to ASK1. Podocytes were incubated with 1 mM AICAR or 5 mM metformin for 2 h before exposing to 1 μg/ml ADR for an additional 1.5 h. Cellular lysates were immunoprecipitated with ASK1 and immunoblotted for Trx and ASK1. Densitometric analyse of Trx is shown at the bottom. Data are expressed as percentage of the untreated

Molecular Pharmacology Fast Forward. Published on December 30, 2013 as DOI: 10.1124/mol.113.089458
This article has not been copyedited and formatted. The final version may differ from this version.

control. (B) Effects of AMPK activators on Trx and ASK1 protein levels. A part of cellular lysate used in A was subjected for Western analysis of ASK1 and Trx. (C, D) Effects of AMPK activators on Trx reductase activity. Podocytes were exposed to 1 mM AICAR or 5 mM metformin for indicated time intervals. Cellular lysates were assessed for Trx reductase activities (mean ± SE, n = 10; * $P < 0.05$ compared with control). (E, F) Effects of AMPK activators on AMPK, Trx and TXNIP. Podocytes were incubated with 1 mM AICAR or 5 mM metformin for the indicated time intervals. Cellular lysates were subjected to Western blot analysis for phosphorylated AMPK, Trx and TXNIP. Densitometric analyses of TXNIP are shown at F. Data are expressed as percentage of control.

Figure 6. Implication of Trx and TXNIP in adriamycin-induced renal tubular cell injury. (A) Induction of cell shape change by ADR. NRK E52 cells were exposed to 2.5 μg/ml ADR for 24 h. Cell morphology was photographed using phase-contrast microscopy (Magnification, ×100). (B) Effect of ADR on cell viability. NRK E52 cells were exposed to the indicated concentrations of ADR for 24 h. The cell viability was evaluated by WST assay. Data are expressed as percentage of living cells against the untreated control (mean ± SE, n = 4; # $P < 0.01$ *versus* zero point). (C) Activation of caspase-3 by ADR. NRK E52 cells were exposed to 2.5 μg/ml ADR for 12 h and subjected to Western blot analysis of caspase-3. The top band represents procaspase-3 (Mr 35,000) and the bottom band indicates its cleaved, mature form (Mr 17,000). (D) Downregulation of Trx and TXNIP by siRNA treatment. NRK-E52 cells were transiently transfected with siRNA against Trx or TXNIP for 48 h. Cell proteins were extracted and subjected to Western blot analysis of Trx and TXNIP. (E-G) Effect of Trx siRNA on cellular viability and P38 activation. NRK-E52 cells were transfected with either Trx siRNA or control siRNA for 48 h. The cellular viability was evaluated through PI staining (E) and formazan formation (F). Data in F are expressed as percentage of living cells, compared with the siRNA control (mean ± SE, n = 4; # $P < 0.01$ *versus* siRNA control).

Molecular Pharmacology Fast Forward. Published on December 30, 2013 as DOI: 10.1124/mol.113.089458
This article has not been copyedited and formatted. The final version may differ from this version.

(G) The cellular lysates were subjected to Western blot analysis for phosphorylated P38. (H) Effect of Trx siRNA on ADR-induced cell injury. NRK-E52 cells were transfected with either Trx siRNA or control siRNA for 48 h and then exposed to 2.5 μg/ml ADR for an additional 24 h. The cell viability was evaluated by WST assay. Data are expressed as percentage of living cells against the untreated control (mean ± SE, n = 4; * $P < 0.05$ *versus* respective control). (I, J) Effect of TXNIP siRNA on ADR-induced cell injury. NRK-E52 cells were transfected with either TXNIP siRNA or control siRNA for 48 h and then exposed to 2.5 μg/ml ADR for an additional 24 h. The cellular viability was through PI staining (I) and formazan formation (J). Data in J are expressed as percentage of living cells, compared with the untreated control (mean ± SE, n = 4; *$P < 0.05$, #$P < 0.01$ *versus* respective control). (K) Effect of TXNIP siRNA on ADR-induced P38 activation. NRK-E52 cells were transfected with either TXNIP siRNA or control siRNA for 48 h and then incubated with or without 1 μg/ml ADR for an additional 6 h. Cellular lysates were subjected to Western blot analysis for phosphorylated P38.

Figure 7. Schematic depiction of the signaling mechanisms involved in the antioxidative effect of AMPK. ADR induces ROS production, which oxidizes Trx and dissociates Trx from ASK1, leading to activation of ASK1-P38 signaling pathway and causing cell damage. AMPK activation promotes Trx binding to ASK1, thus suppressing ASK1-P38 signaling pathway. This effect of AMPK was achieved, on the one hand, through enhancing Trx reductase activities that convert oxidized Trx to reduced form; and on the other hand, through suppressing TXNIP that inhibits Trx activities by binding to reduced Trx.

Figure 1

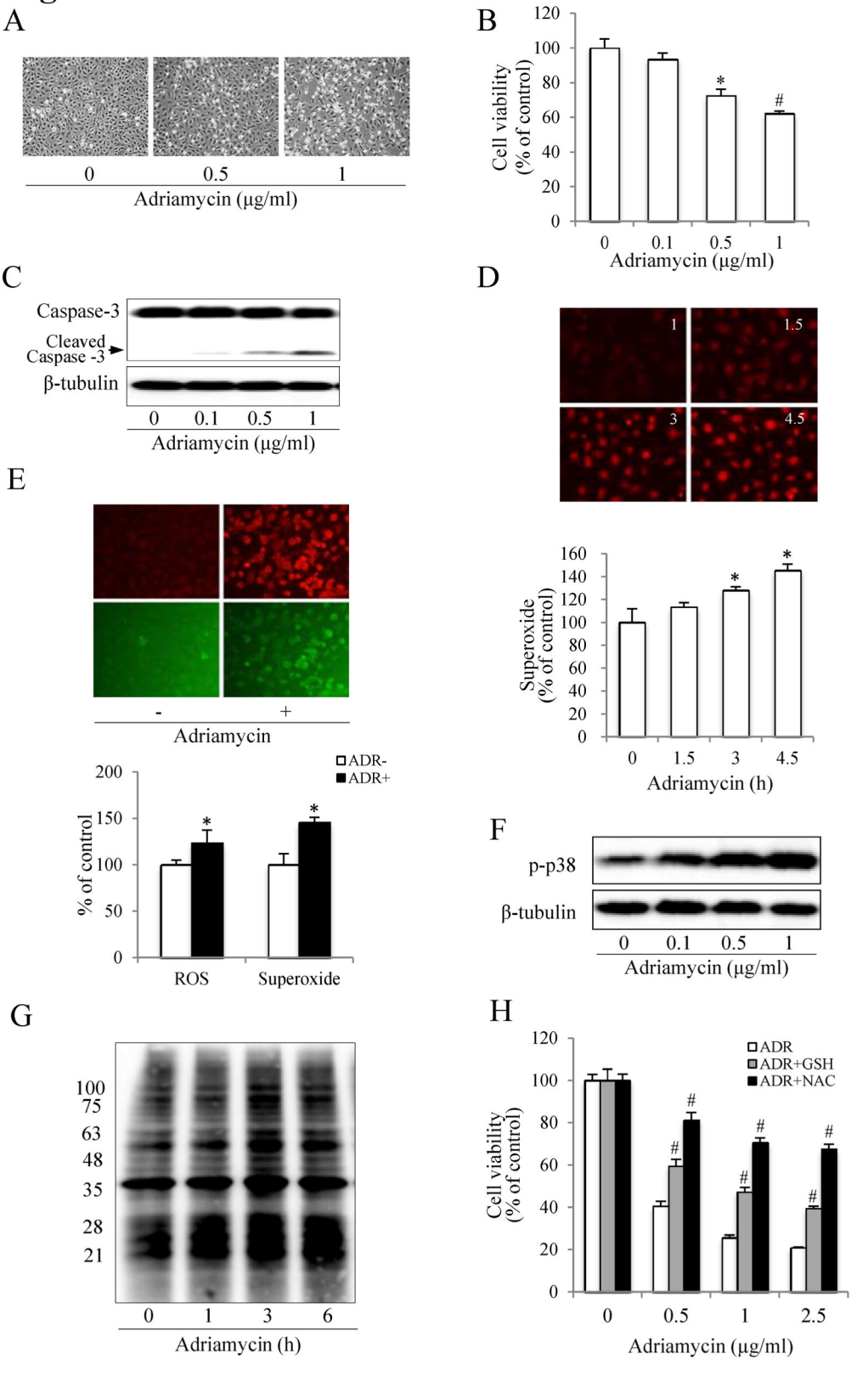
A
0
0.5
1
Adriamycin (μg/ml)
B
Cell viability (% of control)
120
100
80
60
40
20
0
*
#
0
0.1
0.5
1
Adriamycin (μg/ml)
C
Caspase-3
Cleaved Caspase -3
β-tubulin
0
0.1
0.5
1
Adriamycin (μg/ml)
D
1
1.5
3
4.5
Superoxide (% of control)
160
140
120
100
80
60
40
20
0
*
*
0
1.5
3
4.5
Adriamycin (h)
E
-
+
Adriamycin
ADR-
ADR+
% of control
200
150
100
50
0
*
*
ROS
Superoxide
F
p-p38
β-tubulin
0
0.1
0.5
1
Adriamycin (μg/ml)
G
100
75
63
48
35
28
21
0
1
3
6
Adriamycin (h)
H
Cell viability (% of control)
120
100
80
60
40
20
0
ADR
ADR+GSH
ADR+NAC
#
0
0.5
1
2.5
Adriamycin (μg/ml)

Figure 2

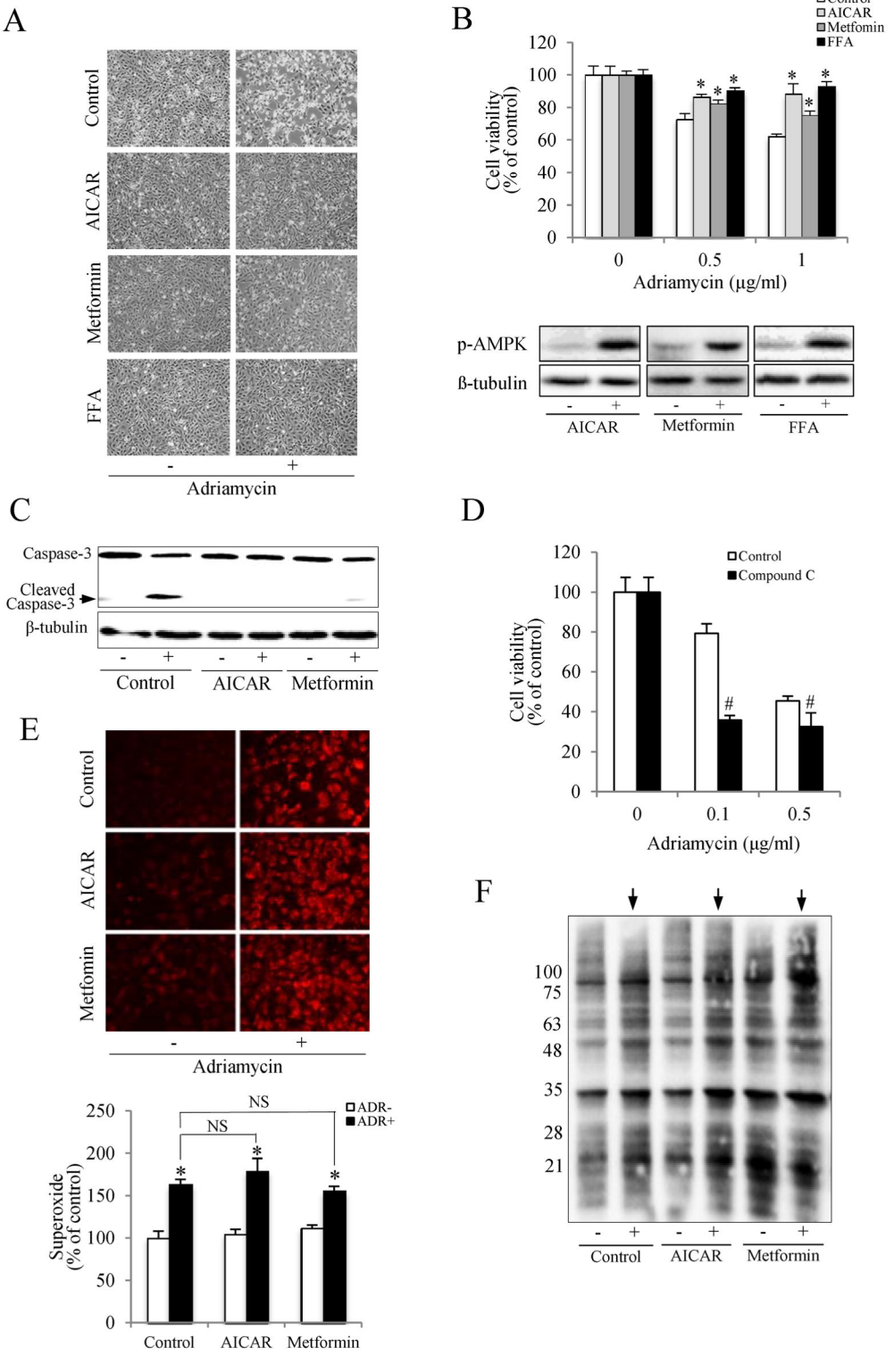
A
Control
AICAR
Metformin
FFA
-
+
Adriamycin
B
Control
AICAR
Metfomin
FFA
Cell viability (% of control)
120
100
80
60
40
20
0
0
0.5
1
Adriamycin (μg/ml)
p-AMPK
ß-tubulin
- + - + - +
AICAR
Metformin
FFA
C
Caspase-3
Cleaved Caspase-3
β-tubulin
- + - + - +
Control
AICAR
Metformin
D
Control
Compound C
Cell viability (% of control)
120
100
80
60
40
20
0
#
#
0
0.1
0.5
Adriamycin (μg/ml)
E
Control
AICAR
Metfomin
-
+
Adriamycin
ADR-
ADR+
NS
NS
Superoxide (% of control)
250
200
150
100
50
0
Control
AICAR
Metformin
F
100
75
63
48
35
28
21
- + - + - +
Control
AICAR
Metformin

Figure 3

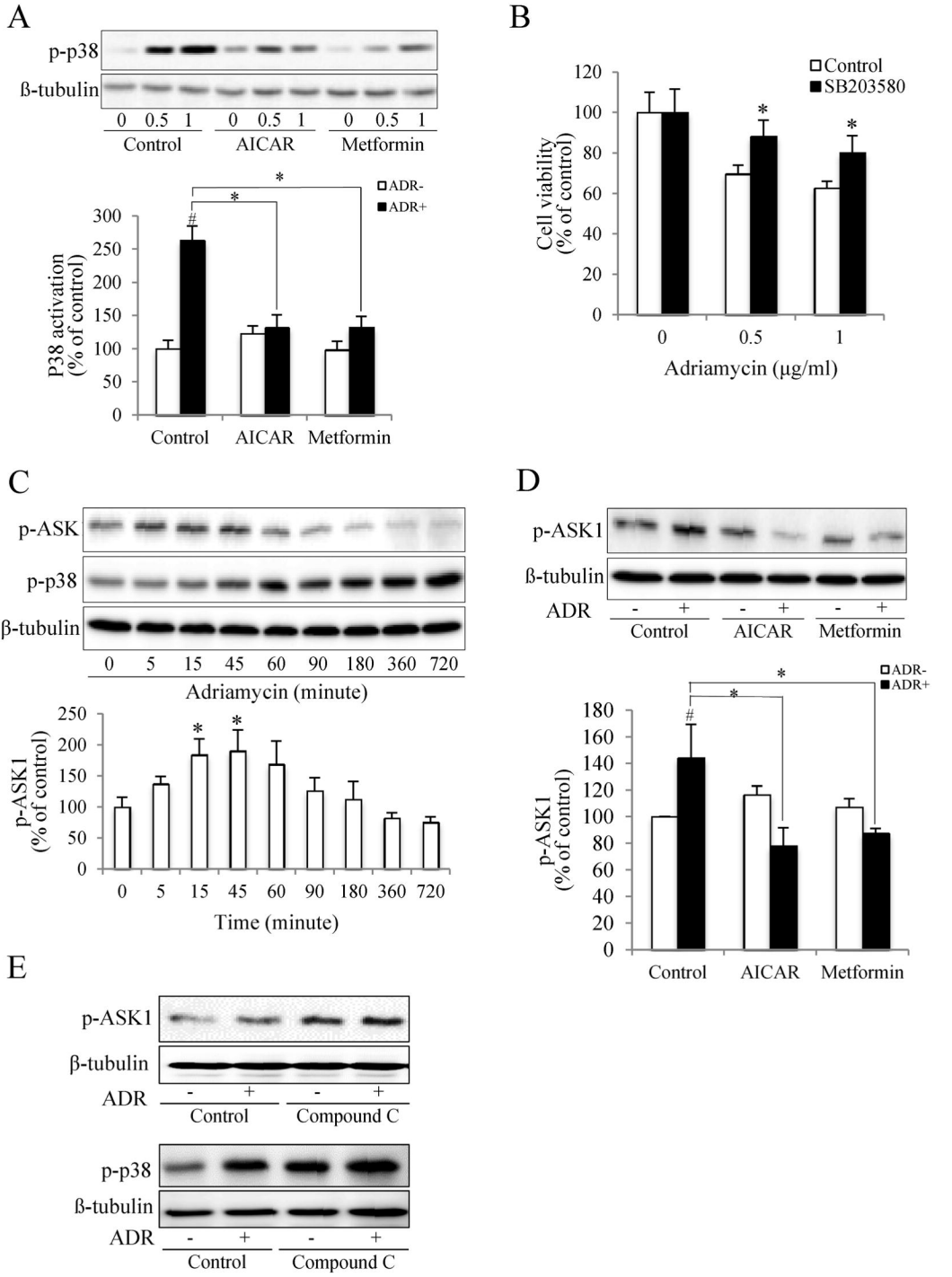
A
p-p38
ß-tubulin
0 0.5 1 0 0.5 1 0 0.5 1
Control
AICAR
Metformin
ADR-
ADR+
P38 activation (% of control)
B
Control
SB203580
Cell viability (% of control)
Adriamycin (μg/ml)
C
p-ASK
p-p38
β-tubulin
0 5 15 45 60 90 180 360 720
Adriamycin (minute)
p-ASK1 (% of control)
Time (minute)
D
p-ASK1
ß-tubulin
ADR
E
p-ASK1
β-tubulin
Compound C
p-p38
ß-tubulin

Figure 4

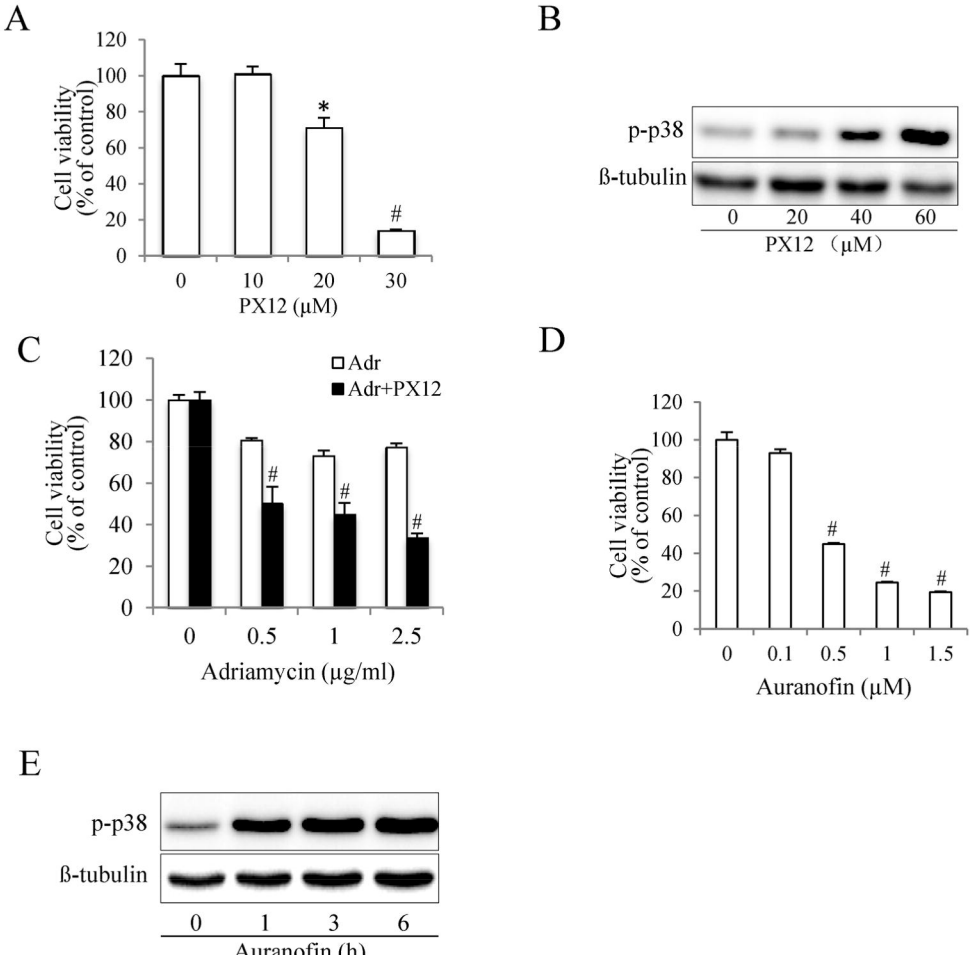
A
Cell viability (% of control)
120
100
80
60
40
20
0
*
#
0
10
20
30
PX12 (μM)
B
p-p38
ß-tubulin
0
20
40
60
PX12 （μM）
C
Adr
Adr+PX12
Cell viability (% of control)
#
0
0.5
1
2.5
Adriamycin (μg/ml)
D
Cell viability (% of control)
#
0
0.1
0.5
1
1.5
Auranofin (μM)
E
p-p38
ß-tubulin
0
1
3
6
Auranofin (h)

Figure 5

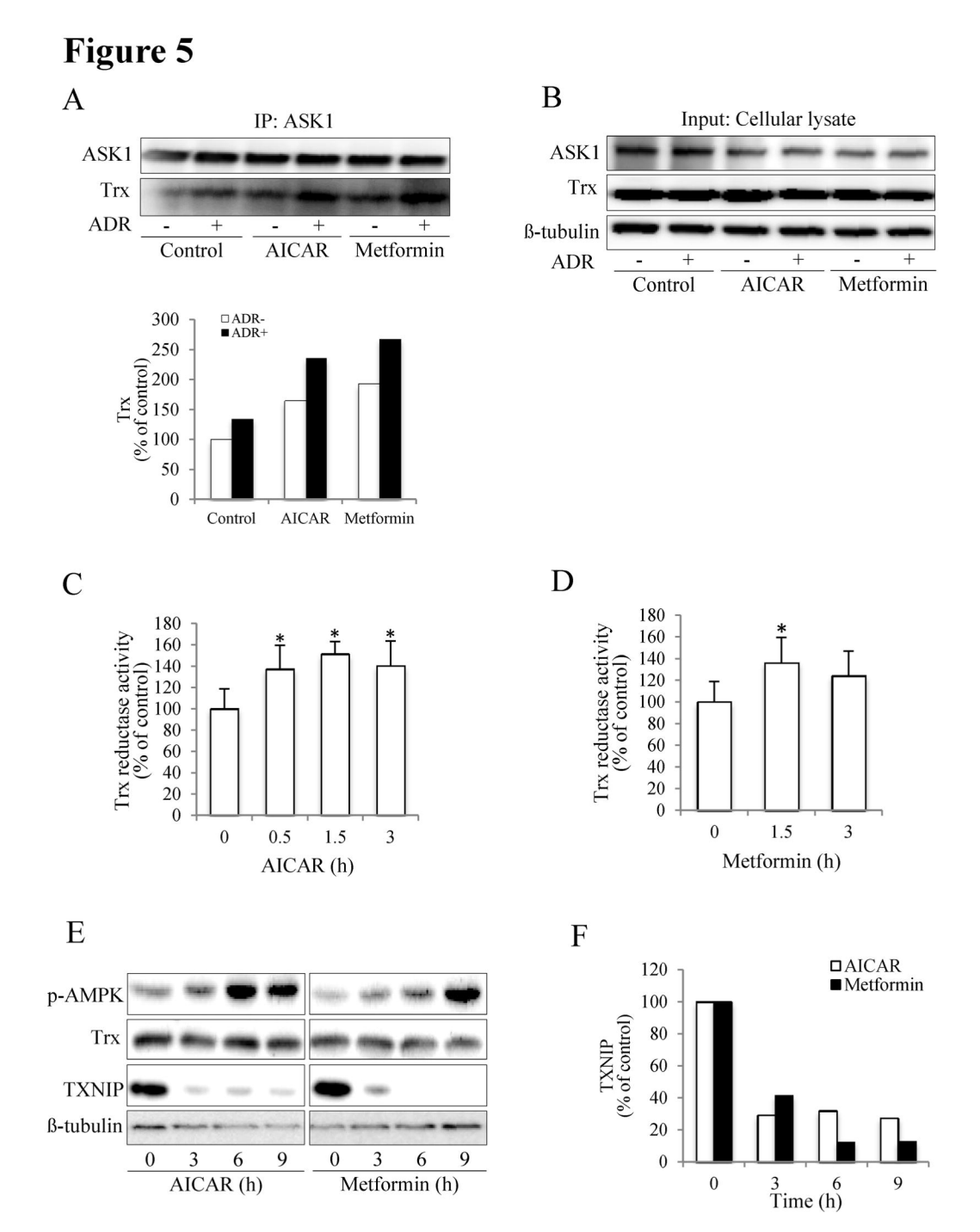
A
IP: ASK1
ASK1
Trx
ADR
- + - + - +
Control
AICAR
Metformin
B
Input: Cellular lysate
ASK1
Trx
ß-tubulin
ADR
- + - + - +
Control
AICAR
Metformin
300
250
200
150
100
50
0
ADR-
ADR+
Trx
(% of control)
Control
AICAR
Metformin
C
Trx reductase activity
(% of control)
180
160
140
120
100
80
60
40
20
0
*
*
*
0
0.5
1.5
3
AICAR (h)
D
Trx reductase activity
(% of control)
180
160
140
120
100
80
60
40
20
0
*
0
1.5
3
Metformin (h)
E
p-AMPK
Trx
TXNIP
ß-tubulin
0 3 6 9 0 3 6 9
AICAR (h)
Metformin (h)
F
120
100
80
60
40
20
0
AICAR
Metformin
TXNIP
(% of control)
0
3
6
9
Time (h)

Figure 6

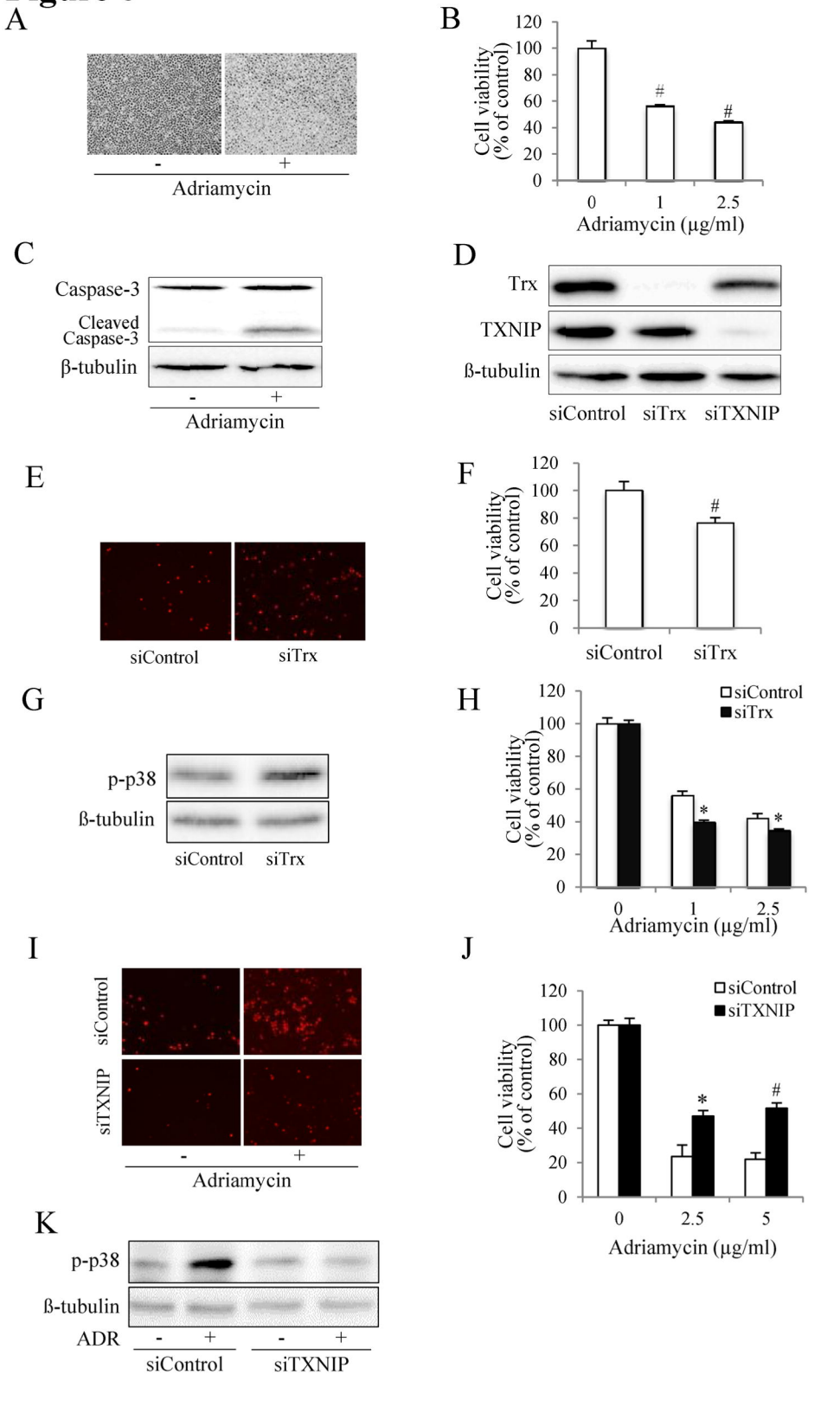
A
-
+
Adriamycin
B
Cell viability (% of control)
120
100
80
60
40
20
0
#
#
0
1
2.5
Adriamycin (μg/ml)
C
Caspase-3
Cleaved Caspase-3
β-tubulin
-
+
Adriamycin
D
Trx
TXNIP
ß-tubulin
siControl
siTrx
siTXNIP
E
siControl
siTrx
F
Cell viability (% of control)
120
100
80
60
40
20
0
#
siControl
siTrx
G
p-p38
ß-tubulin
siControl
siTrx
H
siControl
siTrx
Cell viability (% of control)
120
100
80
60
40
20
0
*
*
0
1
2.5
Adriamycin (μg/ml)
I
siControl
siTXNIP
-
+
Adriamycin
J
siControl
siTXNIP
Cell viability (% of control)
120
100
80
60
40
20
0
*
#
0
2.5
5
Adriamycin (μg/ml)
K
p-p38
ß-tubulin
ADR
-
+
-
+
siControl
siTXNIP

Figure 7

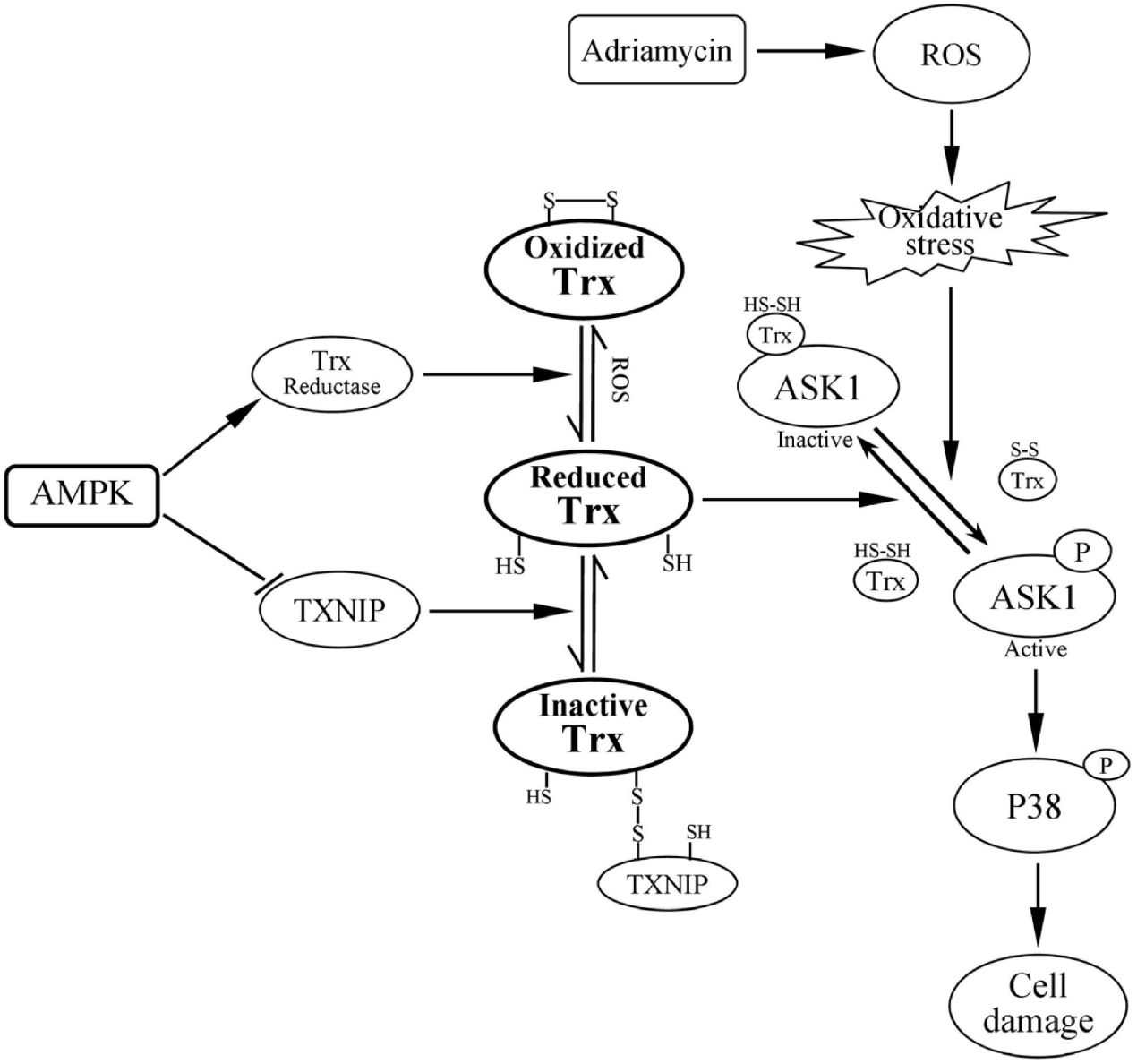
Adriamycin
ROS
Oxidative stress
S—S
Oxidized Trx
HS-SH
Trx
ASK1
Inactive
Trx Reductase
ROS
AMPK
Reduced Trx
HS
SH
S-S
Trx
HS-SH
Trx
P
ASK1
Active
TXNIP
Inactive Trx
HS
S
S
SH
TXNIP
P
P38
Cell damage